Asian Journal of Convergence in Technology **Volume IV Issue II**
ISSN NO: 2350-1146 I.F-5.11

A Novel Modified P-Q Theory to Control PV-UPQC under Power Quality Issues in Distribution System

J. Sandhya Rani,
PG Scholar, M. Tech (EPS), VNR Vignana Jyothi Institute of Engineering and Technology (Autonomous), Hyderabad, sandy.jyothi7@gmail.com

Dr. Rashmi Kapoor
Asst. Professor, Department of Electrical and Electronics Engineering, VNR Vignana Jyothi Institute of Engineering and Technology (Autonomous), Hyderabad, rashmi_k@vnrvjiet.in

***Abstract*- This paper deals with the design and performance analysis of a three-phase single stage solar photovoltaic integrated unified power quality conditioner (PV-UPQC). The PV-UPQC consists of a shunt and series connected voltage compensators connected back to back with common DC-link. The shunt compensator performs the dual function of extracting power from PV array apart from compensating for load current harmonics. The system incorporates clean energy generation along with power quality improvement thus increasing functionality of the system. The fundamental frequency positive sequence (FFPS) components of voltages at the point of common coupling (PCC) are extracted using generalized cascaded delay signal cancellation (GCDSC) technique which are then used in p-q theory based control to estimate reference signals for the PV-UPQC. The series compensator compensates for the grid side power quality problems such as grid voltage sags/swells. The compensator injects voltage in-phase/out of phase with point of common coupling (PCC) voltage during sag and swell conditions respectively. The proposed system combines both the benefits of clean energy generation along with improving power quality. The steady state and dynamic performance of the system are evaluated by simulating in Matlab/Simulink under various loading conditions like nonlinear load, Induction motor, sudden changes in loads connected and faults.**

***Index Terms*- Distribution system, Power Quality, Sag/Swell, Non-Linear load, PV-UPQC, PCC**

I. INTRODUCTION

There is an increased integration of renewable energy systems such as solar PV energy and wind energy into modern distribution systems owing to its benefits of being environmental friendly. However, these sources of energy are intermittent in nature. The loads present in modern distribution system are mainly power electronics based loads which are highly nonlinear. The increased installation of renewable energy sources and nonlinear loads result in several power quality problems both at load side and grid side[1].

As renewable energy sources like solar PV energy are intermittent, their increased penetration in distribution systems leads to voltage quality problems like voltage sags/swells, interruption, flicker and eventually instability in the grid. These voltage quality problems can also lead to frequent false tripping of power electronic systems, malfunctioning and false triggering electronic systems and increased heating of capacitor banks etc [2]–[4]. Current quality issues are mainly caused by the nonlinear loads connected in the distribution systems. These nonlinear loads inject harmonics into distribution system. These harmonics in current lead to distortion of point of coupling (PCC) voltage especially in weak grids apart from causing losses in distribution cables and transformers.

With the advancement in semiconductor technology, there is an increased penetration of power electronic loads. These loads such as computer power supplies, adjustable speed drives, swtiched mode power supplies etc. have very good efficiency, however, they draw nonlinear currents. These nonlinear currents cause voltage distortion at point of common coupling particularly in distribution systems. There is also increasing emphasis on clean energy generation through installation of rooftop PV systems in small apartments as well as in commercial buildings. However, due to the intermittent nature of the PV energy sources, an increased penetration of such systems, particularly in weak distribution systems leads to voltage quality problems like voltage sags and swells, which eventually instability in the grid. These voltage quality problems also lead to frequent false tripping of power electronic systems, malfunctioning and false triggering of electronic systems and increased heating of capacitor banks etc. Power quality issues at both load side and grid side are major problems faced by modern distribution systems[2]-[4].

Due to the demand for clean energy as well as stringent power quality requirement of sophisticated electronic loads, there is need for multifunctional systems which can integrate clean energy generation along with power quality improvement. A three phase multi-functional solar energy conversion system, which compensates for load side power quality issues has been proposed.. A single phase solar pv inverter along with active power filtering capability has been proposed in. Major research work has been done in integrating clean energy generation along with shunt active filtering. Though shunt active filtering has capability for both load voltage regulation, it comes at the cause of injecting reactive power. Thus shunt active filtering cannot regulate PCC voltage as well as maintain grid current unity power factor at same time. Recently, due to the stringent voltage quality requirements for sophisticated electronics loads, the use of series active filters has been proposed for use in small apartments and commercial building. A solar photovoltaic system integrated along with dynamic voltage restorer has been proposed in. Compared to shunt and series active power filters, a unified power quality conditioner (PV-UPQC), which has both series and shunt compensators can perform both load voltage regulation and maintain grid current sinusoidal at unity power factor at same time. Integrating PV array along with PV-UPQC, gives the dual benefits of clean energy generation along with universal active. The integration of PV array with PV-UPQC has been reported in. Compared to conventional grid connected inverters, the solar PV integrated PV-UPQC has numerous benefits such as improving power quality of the grid, protecting critical loads from grid side disturbances apart from increasing the fault ride through capability of converter during transients. With the increased emphasis on distributed generation and microgrids, there is a renewed interest in PV-UPQC systems[4].

Reference signal generation is a major task in control of PV-UPQC. Reference signal generation techniques can be broadly divided into time-domain and frequency domain techniques. Time domain techniques are commonly used because of lower computational requirements in real-time implementation. The commonly used techniques include instantaneous reactive power theory (p-q theory), synchronous reference frame theory (d-q theory) and instantaneous symmetrical component theory. The main issue in use of synchronous reference frame theory based method is that during load unbalanced condition, double harmonic component is present in the d-axis current. Due to this, low pass filters with very low cut off frequency is used to filter out double harmonic component.

The methods based on p-q and d-q theories that are used for calculating the reference signal in the earlier times were largely time domain based techniques. Apart from traditional d-q and p-q theories[5]-[7] there are other advanced control methods for generating the reference signal which use the adaptive filters such as adaptive notch

filter(ANF), Adaptive Linear Element(ADALINE) etc[10]-[12]. But these methods need calculation for each phase currents and voltages which makes more complex when compared to p-q and d-q theories. However the conventional p-q theory is not able to generate accurate results in the case of voltage distortions or unbalanced conditions. This disadvantage can be overcome by using fundamental frequency positive sequence (FFPS) voltages for the calculation of reference current signal. For this purpose the modified p-q theory use the Generalized Cascaded Delay Signal Cancellation (GCDSC) technique.

In this paper, the design and performance analysis of a three phase PV-UPQC are presented. An modified p-q theory based control is used to improve the dynamic performance during load active current extraction. The main advantages of the proposed system are as follows,

• Integration of clean energy generation and power quality improvement.
• Simultaneous voltage and current quality improvement.
• Improved load current compensation due to use of GCDSC control of PV-UPQC.
• Stable under various dynamic conditions of voltage sags/swells, load unbalance and irradiation variation.

The performance of the proposed system is analyzed extensively under both dynamic and steady state conditions using Matlab-Simulink software.

II. SYSTEM DESCRIPTION

The structure of the PV-UPQC is shown in Fig.1. The PV-UPQCis designed for a three-phase system. The PV-UPQC consists of shunt and series compensator connected with a common DC-bus. The shunt compensator is connected at the load side. The solar PV array is directly integrated to the DC-link of PV-UPQC through a reverse blocking diode. The series compensator operates in voltage control mode and compensates for the grid voltage sags/swells. The shunt and series compensators are integrated to the grid through interfacing inductors. A series injection transformer is used to inject voltage generated by the series compensator into the grid. Ripple filters are used to filter harmonics generated due to switching action of converters. The loads used are a nonlinear load consisting of a bridge rectifier with a voltage-fed load, an R-load, Induction motor for analyzing various power quality problems apart from regular linear load.

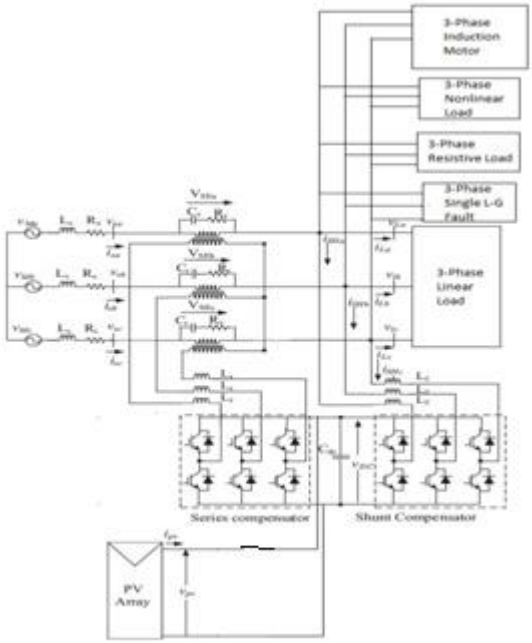

Fig.1 System Configuration PV-UPQC

The distribution system shown in figure1 is connected to various types of loads through the line impedance. The loads are linear load, non-linear load and sensitive loads. The sensitive load in this case refers to RL load. A Single line to Ground fault is also placed in the system at a particular point of time to study the case of unbalance. The issues like harmonics, Sag/Swell conditions and unbalanced cases are as described below.

The increasing usage of power electronic converters and semiconductor devices, causes the power system to be subjected to harmonics especially the deterioration of current profile is insisting the concern towards power quality problem. A three phase diode bridge rectifier with

R-L load across its output terminals is used as non-linear load in the system.

A three phase asynchronous machine i.e, induction motor is connected to the system. As we know Induction motor needs high starting torque so initially it draws the huge current from the source there by causing a dip in the voltage which is called as sag. The voltage comes to the normal state automatically once the motor achieves the rated speed but the sag in the source voltage is not the desired one so it must be either eliminated or reduced.

The power system is subjected to load changes often. The sudden trip or outage of the load may cause rise in the voltage which is called as swell.

A single Line to Ground fault is placed in the system to create unbalance in the source voltages and load voltages as well.

The phasor diagram of the PV-UPQC with a linear reactive load is presented in Fig. 2. The subscript '1' represents condition when reactive power is shared by shunt VSC only whereas the subscript '2' refers to condition when the series VSC shares a part of reactive load power. The PCC voltage (*VS*1) and load voltage (*VL*1) are in phase when series VSC is not injecting any voltage. The load current before series compensation is (*IL*1) and the load angle is (φ). The shunt VSC also injects real power obtained from PV array which is represented by (*IPV*). The remaining part of the load real power is obtained from the grid (*IS*1). The shunt VSC current (*ISH*1) before series VSC injection is phasor sum of PV array current and load reactive current. When a part of reactive power of the load is to be shared by series VSC, then series VSC injects voltage (*VSE*) such that load voltage is shifted to (*VL*2). This results in shifting of load current to (*IL*2). However, as the active current drawn from the grid is to remain same (*IS*1 = *IS*2 = *IS*), the shunt VSC current reduces to (*ISH*2). It can observed that due to power angle (δ), the part of reactive burden of shunt VSC is shared by the series VSC thus increasing the utilization of series VSC[1].

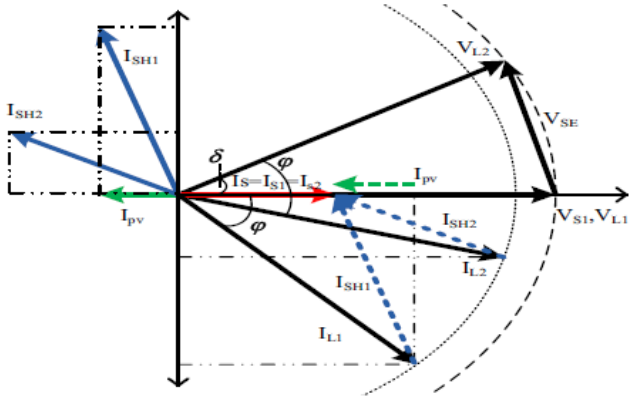

Fig. 2. Phasor Diagram of PV-PV-UPQC

A. Photovoltaic Unified Power Quality Conditioner

PV-UPQC-Unified Power Quality Conditioner, a FACTS family device of series-shunt type. The circuitry of PV-UPQC is also shown in the figure1. It is constructed as a combination of two voltage source converters i.e, series converter and shunt converter which share the common DC link(A capacitor connected in between the series and shunt converters)[3]. PV is connected across DC-link.

The series converter is used mainly for voltage compensation as it either injects the voltage in to the system or draws the voltage from the main system and shunt converter is used for load side compensation which either injects the current into or takes the current from, the main distribution system. The shunt converter also regulates the common DC-link voltage and also it acts as Active Power Filter which compensates the current harmonics. It balances the reactive power and improves the power quality of the distribution system. The detailed description of control strategies is presented in section III.

B. Design of PV-PV-UPQC

The design procedure for PV-UPQC begins with the proper sizing of PV array, DC-link capacitor, DC-Link voltage level etc. The shunt compensator is sized such that it handles the peak power output from PV array apart from compensating for the load current reactive power and current

harmonics. The specifications of solar PV module used to realize PV array is given in Table-I. The PV array rating is selected as 16.2kW as given in Table-I. The rating is such that, under nominal conditions the PV array supplies around half of the load active power and remaining load active power is drawn from the grid. The other components to be designed are the interfacing inductors of series and shunt compensators and series injection transformer of the series compensator. The design of PV-UPQC is further elaborated as follows[13].

1) PV Array: As the PV array is directly integrated to the DC-link of PV-UPQC, the PV array is sized such that the MPP voltage is same as desired DC-link voltage. The PV module is based on Solar Module SunPower SPR-305-WHT. The solar PV array is made with a combination of series and parallel strings where 4 parallel strings and 13 modules for each series string are inserted. The SPV array specification is given in Table-I.

TABLE I
SOLAR PV ARRAY SPECIFICATIONS

Parameter	Value
Maximum Power(P)	16.2KW
Open Circuit Voltage(V*oc*)	875V
Short Circuit Current(I*sc*)	24.63A
Voltage at Maximum Power Point(V*mpp*)	704V
Current at Maximum Power Point(I*mpp)*	23A
Parallel Strings	
Series Modules per	

2) Voltage Magnitude of DC-Link: The magnitude of DClink voltage Vdc depends on the depth of modulation used and per-phase voltage of the system. The DC-link voltage magnitude should more than double the peak of per-phase voltage of the three phase system and is given as,

$$V_{dc} = \frac{2\sqrt{2}V_{LL}}{\sqrt{3}m} \quad (1)$$

where depth of modulation (m) is taken as 1 and VLL is the grid line voltage. For a line voltage of 415V, the required minimum value DC-bus voltage is 677.7V. The DC-bus voltage is set at 700V(approx) which is same as the MPPT operating voltage of SPV array at STC conditions.

3) DC-Bus Capacitor Rating: The DC-link capacitor is sized based upon power requirement as well as DC-bus voltage level. The energy balance equation for the DC-bus capacitor is given as follows

$$C_{dc} = \frac{3kaV_{ph}I_{sha}t}{0.5\times(V_{dc}^2 - V_{dc1}^2)} \quad (2)$$

where Vdc is the average DC-bus voltage, $Vdc1$ is the lowest required value of DC-bus voltage,a is the overloading actor, Vph is per-phase voltage, t is the minimum time required for attaining steady value after a disturbance, Ish is per-phase current of shunt compensator, k factor considers variation in energy during dynamics.

4) Interfacing Inductor for Shunt Compensator: The interfacing inductor rating of the shunt compensator depends upon the ripple current, the switching frequency and DC-link voltage. The expression for the interfacing inductor is as,

$$L_f = \frac{\sqrt{3}mV_{dc}}{12af_{sh}I_{crpp}} \quad (3)$$

where m is depth of modulation, a is pu value of maximum
overload, $fsh$is the switching frequency , Icr,pp is the inductor ripple current which is taken to be 20% of rms phase current of shunt compensator.

5) Series injection Transformer: The series compensator is designed for compensating a maximum voltage sag/swell of 0.3pu and hence the required voltage to be injected is only 69V. The series compensator operates at low modulation index for 415V DC-link voltage which results in increased harmonics. In order to keep modulation index of series VSC near to unity, a series injection transformer is used turns ratio is given as,

$$K_{SE} = \frac{V_{vsc}}{V_{SE}} \quad (4)$$

6) Interfacing Inductor of series compensator: The rating of interfacing inductor of series compensator depends upon the ripple current at swell condition, switching frequency and DC-link voltage and series injection transformer turns ratio.

Its value is expressed as,

$$L_r = \frac{mV_{dc}K_{SE}}{4af_sI_r} \quad (5)$$

where m is the depth of modulation, a is the pu value of maximum overloading, fs is the series compensator switching frequency, Ir is the inductor current ripple at swell condition, which is taken to be 20% of grid current.

III. CONTROL OF PV-UPQC

The main subsystems of PV-UPQC are the shunt compensator and the series compensator. The shunt compensator compensates for the load power quality problems such as load current harmonics and load reactive power. In case of PV-UPQC, the shunt compensator performs the additional function of supplying power from the solar PV array. The shunt compensator extracts power from the PV-array by using a maximum power point tracking (MPPT) algorithm. The series compensator protects the load from the grid side power quality problems such as voltage sags/swells by injecting appropriate voltage in phase with the grid voltage.

A. Generalized Cascaded Delay Signal Cancellation Block

The method is based on computing the instantaneous αβ voltage vector and this vector delayed in time. A mathematical transformation is proposed through which the

original and delayed voltage vectors are combined. It is shown that with the proposed generalized cascaded delayed signal cancelation (GCDSC) technique, the transformation may be designed so that the FFPS voltage vector passes through it with unity gain. On the other hand, chosen positive- and negative-sequence harmonics components are eliminated. Cascaded transformations can then be used for accurately obtaining the FFPS voltage vector.

An ideal FFPS voltage vector detector should be able to eliminate the fundamental-frequency negative-sequence vector along with all positive- and negative-sequence harmonic vectors. On the other hand, the gain for the FFPS vector should be equal to one. It is not possible to cancel all harmonic component vectors using only one transformation of the type described in (11). However, some transformations may be chosen to be put in cascade for eliminating harmonic component vectors around the FFPS vector.

As we mentioned above, for the extraction of FFPS signal component of voltage a delay signal cancellation (DSC) operator [10] is used and the equation for the same is given as below,

$$V_{h\alpha\text{-}\beta}(t) = \frac{1}{2}\left[V_{\alpha-\beta}(t) + e^{\frac{j2pi}{N}}V_{\alpha-\beta}\left(t-\frac{T}{N}\right)\right] \quad (6)$$

In the above equation the voltage component vector values are presented in α-β frame, where vα−β(t) = vα + jvβ(t) is the voltage vector, vhα−β(t) = vhα(t) + jvhβ(t) is the FFPS component of voltage which is given in sequentially with different harmonics orders as in the equation h represents harmonic order and the value of h is, h = N ×k+1 (k = ±1,±2,±3...) in α−β domain, T is the fundamental period of voltage, delay factor is N. The DSC operator has a transfer function and its value is given in equation 7 as below,

$$G_N(j\omega) = \left|\cos\left(\frac{\omega T}{2N}-\frac{\pi}{N}\right)\right| \angle\left(\frac{\omega T}{2N}-\frac{\pi}{N}\right) \quad (7)$$

In equation 2, 'N' is known as delay factor and it is used to block the harmonics of the particular order which is given as, $h_b = N \times k - 1$ ($k = \pm1,\pm2,\pm3...$). Using equations 1 and 2, the DSC operator is mathematically modeled and that is depicted in Fig. 3(a). In the figure the delay is shown with the block $z-M$ which is in discrete form where M represents the value of delay sample corresponding to a delay factor of N. As it is difficult to find specifically, the PCC voltage harmonic quantity, the possible solution is to

connect five delay signal operator blocks in series with delay factors N = 2, 4, 8, 16, 32 [4]. This system of series connected blocks is known as GCDSC block which is shown in Fig. 3(b).

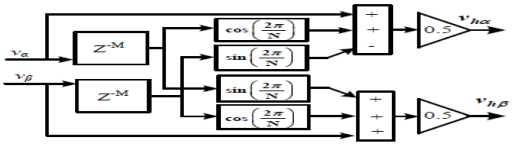

(a) Delay Signal Cancellation Block-N

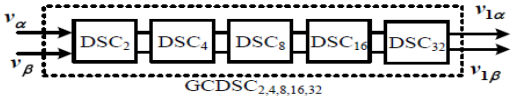

(b) Generalized Cascaded Delay Signal Cancellation Block

Fig.3 Fundamental Frequency Positive Sequence Extraction using Generalized Cascaded Delay Signal operation

As we know, frequency adaptive system is quite effective, this can be done by using the GCDSC block as a pre-filtering mechanism, but it is more complex. The GDSC causes an attenuation in a signal of 0.065% and phase error is observed at a value of 3.43◦(2), where the given signal frequency is 59Hz, if the GDSC is designed for frequency of 60Hz. The grid fundamental frequency varies in a low range where the variation is in between 59.3 and 60.2 Hz in normal conditions, which causes insignificant change in the values of magnitude and phase error. As the changes are insignificant, there is not much necessity of making the system, frequency adaptive so that unnecessary complexity can be avoided.

The function of GCDSC is mainly to extract the FFPS component so it a only allows the same through it but still it is also able perform the operation of attenuating the lower order harmonic values. However, while these lower order harmonics are passing through GCDSC few of them comes out from it without alteration. Such harmonics are measured as $h = 32 \times k + 1$, ($k = \pm1,\pm2..$), (i.e 33*rd* positive sequence harmonic, 31*st* negative sequence harmonic etc.). Usually, the magnitude of such components is not considered. Though these lower order components are insignificant, they are sufficiently able to cause the error in the calculation of magnitude and phase values. Because of this reason a band-pass filter (BPF) is also used to remove these high frequency signals from FFPS signal that is obtained from GCDSC.

B. Load Power Calculation Block

The p-q theory power components are then calculated from voltages and currents in the α-β-*0* coordinates. Each component can be separated in its mean and alternating values,

$\bar{p}$ – Mean value of the instantaneous real power. It corresponds to the energy per time unity that is transferred from the power source to the load, in a balanced way, through the *a-b-c* coordinates (it is, indeed, the only desired power component to be supplied by the power source).

$\tilde{p}$– Alternating value of the instantaneous real power. It is the energy per time unity that is exchanged between the power source and the load, through the *a-b-c* coordinates. Since $\tilde{p}$ does not involve any energy transference from the power source to load, it must be compensated.

$\bar{q}$ – Mean value of instantaneous imaginary power.

$\tilde{q}$ – Alternating value of instantaneous imaginary power.

To get the values of fundamental active power *PL* and reactive power *QL*, the instantaneous active power *pL* and reactive power *qL* are given to a low-pass filter (LPF).

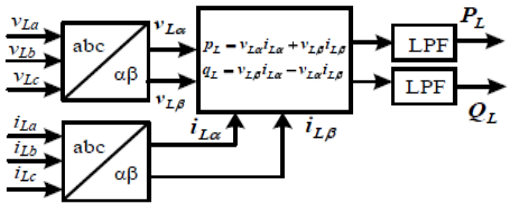

Fig.4 Block diagram of Power Block

The instantaneous imaginary power, *q*, has to do with power (and corresponding undesirable currents) that is exchanged between the system phases, and which does not imply any

transference or exchange of energy between the power source and the load.

C. Shunt VSC Control Structure

The shunt compensator extracts the maximum power from
the solar PV-array by operating it at its maximum power point. The maximum power point tracking (MPPT) algorithm generates the reference voltage for the DC-link of PV-UPQC. Some of the commonly used MPPT algorithms [28] are Perturb and Observe (P& O) algorithm, incremental conductance algorithm (INC). In this work, (P& O) algorithm is used for implementing MPPT. The DC-link voltage is maintained at the generated reference by using a PI-controller[14]-[16].

As it is shown in fig. 5, the shunt converter control strategy starts with transformation of abc voltage quantities into α-β domain quantities. The shunt converter is capable of solving current power quality issues on load side such as unbalanced loading, disturbed current and poor power factor can be mitigated by the shunt VSC. Apart from this, to maintain the DC-bus voltage at required reference value, it injects real power obtained from DC link into the grid. The reference value for the DC-bus voltage is obtained from general relation between RMS and DC offset value of the AC system. The sensed DC-bus voltage (*Vdc*) is passed through LPF and is compared with reference DC-bus voltage (V^*dc). The error between *Vdc* and V^*dc is given to proportional integral (PI)-controller to calculate the loss component (*Ploss*).

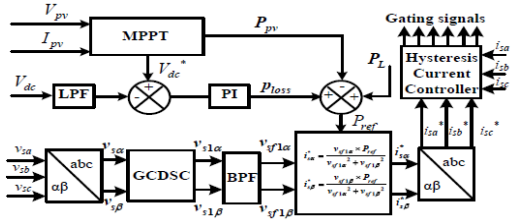

Fig5 Shunt VSC Control Structure

Equation 8 gives the power (*Pref*) to be drawn from the grid which is mentioned below,

$$P_{ref}=P_L+P_{loss} \quad (8)$$

The FFPS components of PCC voltages *vs*1*α, vs*1*β* obtained using GCDSC block are filtered using band pass filters to give *vsf*1*α, vsf*1*β*. The reference grid currents in $\alpha - \beta$ frame are calculated using *Pref*and *vsf*1*α, vsf*1*β* as,

$$i_\alpha^* = \frac{V_{sf1\alpha}*P_{ref}}{V_{sf1\alpha}^2+V_{sf1\beta}^2} (9)$$

$$i_\beta^* = \frac{V_{sf1\beta}*P_{ref}}{V_{sf1\alpha}^2+V_{sf1\beta}^2} (10)$$

The above reference current signals are then again converted back to abc domain and compared with measured grid currents (*isa, isb, isc*) in a hysteresis current controller to produce gating signals for the shunt VSC.

D. Control of Series VSC

The control block diagram of series VSC is shown in Fig5. The series VSC, not only protects the sensitive loads from PCC voltage sags/swells, but also compensates for a part of the load reactive power even under normal PCC voltage conditions. The relationship between power angle δ and reactive power shared by series VSC (*QSE*) under normal condition [10] is given in equation 11,

$$\delta = arcsin[\frac{Q_L - Q_{SH}}{P_L - P_{pv}}] \quad (11)$$

where *QSH* is a standard preset parameter which is the amount of reactive power to be shared by the shunt VSC, *QL* is average load reactive power, *PL* is average load active power and P_{pv} is power from the PV array. Under conditions of PCC voltage sag and swell, the expression is modified as below which is shown in equation 12,

$$\delta = arcsin[\frac{Q_L - Q_{SH}}{K(P_L - P_{pv})}] \quad (12)$$

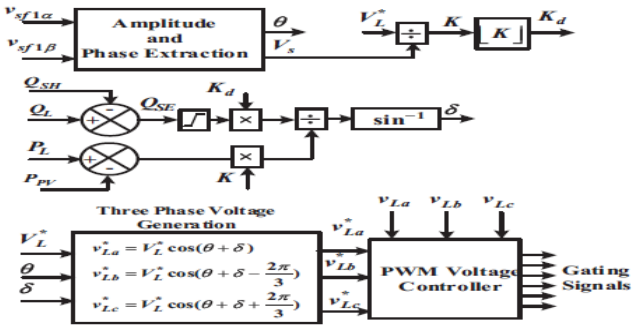

Fig.6 Series VSC Control Structure

where *K* is ratio between load reference voltage peak *VL* and PCC voltage peak *VS*. For the justification of (7). the magnitude of (*QL* − *QSH*) should be always lesser than (*PL* −*Ppv*). The power angle δ is less when P_{pv} is lesser and vice-versa, for same reactive power sharing by series VSC. The peak of PCC fundamental voltage (*VS*) and its phase(θ) are obtained by using *vsf*1α, *vsf*1β components .

The ratio between *VS* and *VL* gives factor *K*. By doing the mathematical operation of 'floor' on *K*, factor *Kd* is calculated. The value of *Kd* is 1 under sag condition and 0 under swell condition. The value of *Kd* is kept 0 under swell condition so that reactive power sharing is done only in sag and nominal conditions because the PCC current decreases under swell condition so a higher amount of voltage needs to be injected for same amount of reactive power compensation, though the series VSC can compensate load reactive power during voltage swell conditions. This requires higher voltage rating of series compensators. As the probability of occurrence of voltage swell is very much lesser as compared to that of voltage sags, it is finalized in the control algorithm to not to give importance to reactive power compensation during swell conditions and it only performs voltage swell compensation. There is a saturation block to keep lower limit of *QSE* to zero. Thus if the load reactive power is less than that of *QSH*, then the entire reactive power is shared by shunt VSC[14]-[16].

The power angle δ is calculated based on (7). Using power angle δ, phase information θ and load voltage reference peak *VL* , the three phase reference load voltages (*vLa, vLb, vLc*) are generated as follows,

$$v^*_{La} = V^*_L \cos(\theta + \delta) \quad (13)$$

$$v^*_{Lb} = V^*_L \cos(\theta + \delta - \frac{2pi}{3}) \quad (14)$$

$$v^*_{Lc} = V^*_L \cos(\theta + \delta + \frac{2pi}{3}) \quad (15)$$

The switching pulses for series VSC are finally produced using a pulse width modulated (PWM) voltage controller which uses the reference load voltages.

IV. TEST SYSTEM SIMULATIONS

The test system i.e, distribution system with PV-UPQC is depicted in Fig.8. The system values are: PCC line voltage: 415 V, 60 Hz; Nonlinear load: Bridge Rectifier with R-L: 10 Ω, 100mH; DC-bus Voltage: 700 V; DC-bus Capacitor: 15 mF; Interfacing Inductor of Shunt VSC: 2mH; Interfacing Inductor of Series VSC: 3mH; DC-bus PI Gains: *Kp*= 1000, *Ki* = 50; LPF cut-off frequency = 10Hz; BPF center frequency = 60Hz, Damping Ratio = 0.7.

To compensate the above mentioned issues which are causing the power quality degradation in the distribution system, at PCC PV-UPQC is connected with necessary control mechanisms.

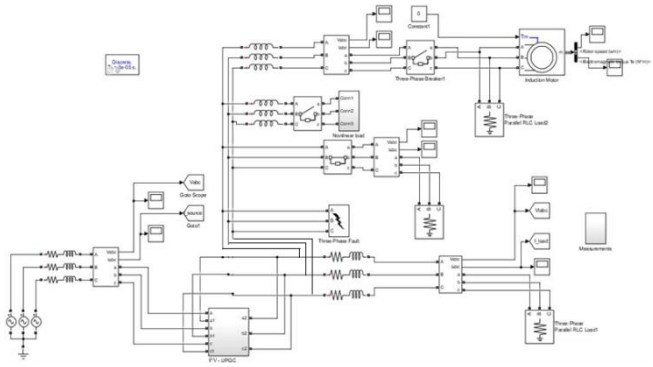

Fig.8 Simulation Configuration of Distribution system with PV-UPQC

V. RESULTS

The Simulation results of various components of the distribution system under different conditions are presented as follows.

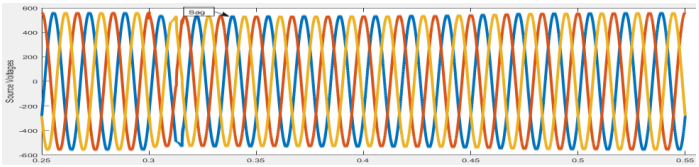

Fig. 9(a) Source Voltages

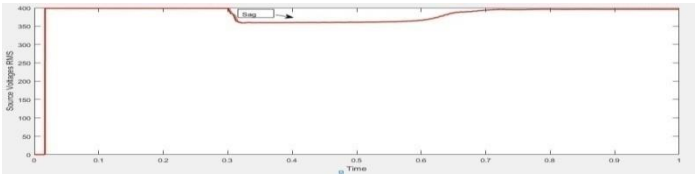

Fig.9(b) Source RMS Voltage

Fig.9(a)shows the source voltages under sag condition, initial peak voltage is 565.6V and when 10HP induction motor is connected at 0.3sec to 0.5secthe effect of sag has begun, and the instantaneous peak voltage is 537V. The percentage of dip in voltage is 7.6%. The same is depicted in the form of RMS value in Fig.9(b), the initial RMS is 400V and instantaneous RMS from 0.3sec to 0.5sec fell down to 380V.

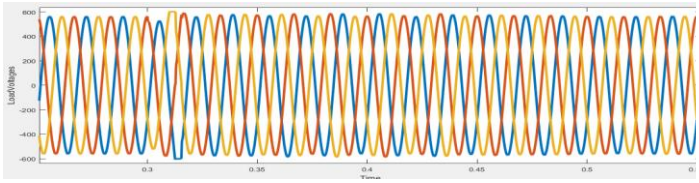

Fig.10(a) Load Voltages

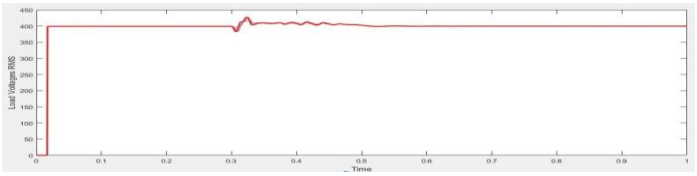

Fig.10(b) Load RMS Voltage

Fig.10(a) shows the load voltages under sag condition. The sag that occurred due to induction motor load has been compensated by connecting PV-UPQC at PCC. The compensation starts from 0.31sec to 0.5sec, due to the transients the delay in PV-UPQC response is 0.01sec and the percentage of compensation is 99.25% as the instantaneous peak voltage during sag is increased to 561.3V where the initial peak voltage is 565V. Fig.10(b) shows the load RMS voltage under sag condition in which the voltage is increased to 397V from 380V during the sag period with a nominal RMS voltage of 400V.

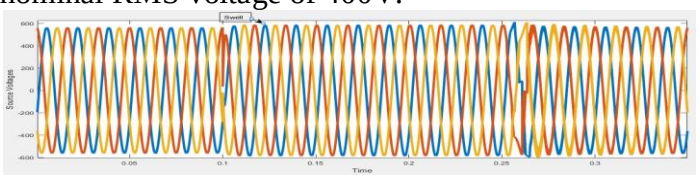

Fig.11(a) Source Voltages

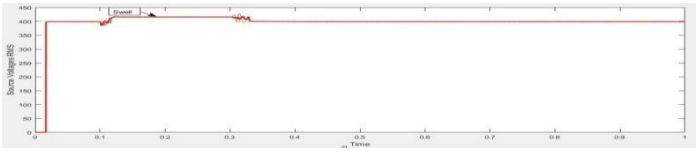

Fig.11(b) Source RMS Voltage

Fig.11(a) shows the source voltages under swell condition, initial peak voltage is 565.6V and when large Resistive load is disconnected at 0.1sec the effect of swell has begun, and the instantaneous voltage is 615V. The percentage of rise in voltage is 8.9%. The same is depicted in the form of RMS value in Fig.11(b), the source RMS is increased from 400V to 435V at 0.1 sec.

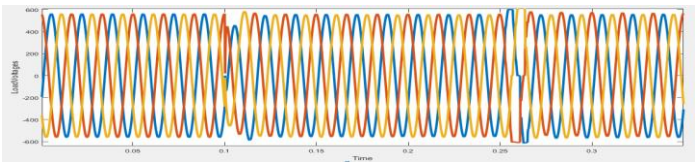

Fig.12(a) Load Voltages

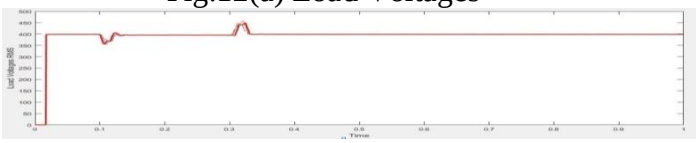

Fig.12(b) Load RMS Voltage

Fig.12(a) shows the load voltages under swell condition. The swell that occurred due to switching off of large resistive load has been compensated by connecting PV-UPQC at PCC. The compensation starts at 0.11sec, due to the transients the delay in PV-UPQC response is 0.01sec and the percentage of compensation is 99.5% as the instantaneous peak voltage during swell is decreased to 566V where the initial peak voltage is 565V. Fig.12(b) shows the load RMS voltage under swell condition in which the voltage is decreased to 398V from 435V during the swell period with a nominal RMS voltage of 400V.

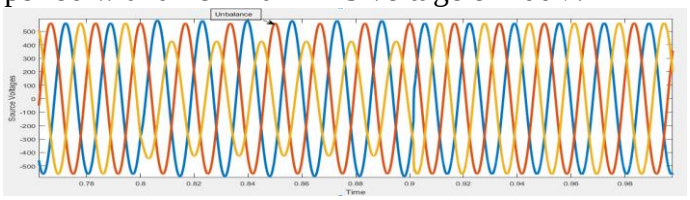

Fig.13(a) Source Voltages:

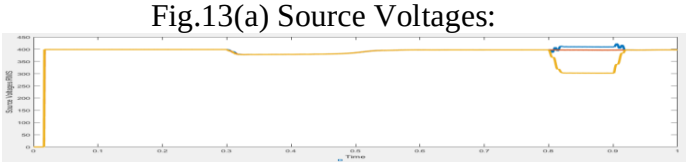

Fig.13(b) Source RMS Voltage

Fig.13(a) shows the source voltages under fault/unbalance condition, initial peak voltage is 565.6V and when a Single Line to ground fault is inserted at 0.8sec the effect of unbalance has begun, and the instantaneous variation in three phase peak voltages is ranges from 537V to 594V. The percentage of variation is ranging from -4.9%to 4.9%. The same is depicted in the form of RMS value in Fig.13(b), the initial RMS is 400V and instantaneous variation in RMS from 0.8sec to 0.9sec is ranges from 380V to 420V.

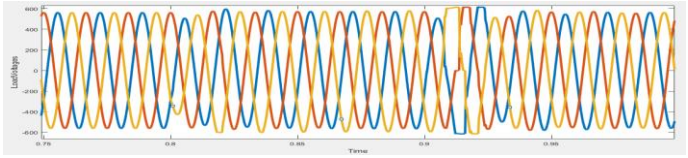

Fig.14(a) Load Voltages

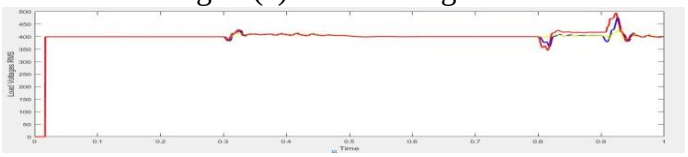

Fig.14(b) Load RMS Voltage

Fig.14(a) shows the load voltages under fault/unbalance condition. The unbalance that occurred due to L-G fault has been compensated by connecting PV-UPQC at PCC. The compensation starts from 0.81sec due to the transients the delay in PV-UPQC response is 0.01sec and the percentage of compensation is 95% as the instantaneous peak voltages during fault, ranges from 558V-574V where the initial peak voltage is 565V. Fig.14(b) shows the load RMS voltage under fault/unbalance condition in which the voltage variation is minimized in the range of 395-406V during the fault period with a nominal RMS voltage of 400V.

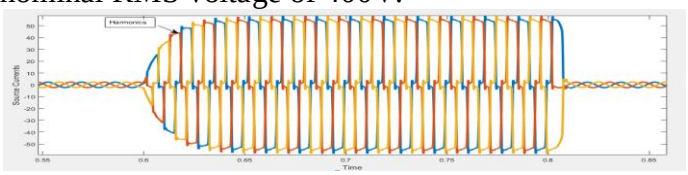

Fig.15(a) Source Currents

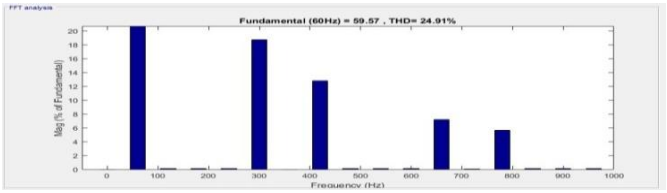

Fig.15(b) THD Spectrum of Source Currents

Fig.15(a) shows the source currents which involve harmonics from 0.6sec to 0.8sec due to the nonlinear load that has been connected at 0.6sec and removed at 0.8sec.Fig15(b) shows the THD spectrum of source currents from FFT analysis and the percentage of Total Harmonic Distortion is 24.92% which is measured at 0.75sec for 1 cycle.

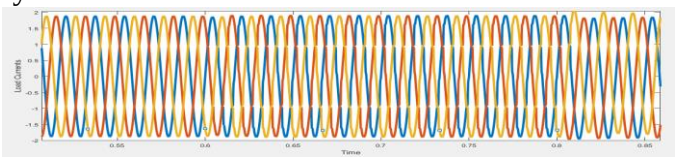

Fig.16(a) Load Currents

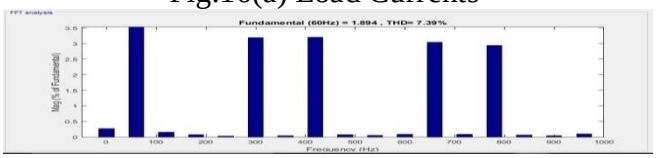

Fig.16(b) THD Spectrum of Load Currents

Fig.16(a) shows the load currents, in which the harmonics that are generated due to nonlinear load are reduced to a permissible level by the active power filter capability of PV-PV-UPQC. Fig16(b) shows the THD spectrum of load currents from FFT analysis and the percentage of Total Harmonic Distortion is 7.38% which is measured at 0.75sec for 1 cycle. The percentage of compensation by PV-UPQC is 17.6%

VI. CONCLUSION

The dynamic performance of three-phase PV-UPQC has been analyzed with constant irradiation under grid voltage sags/swells and also under fault conditions. It is observed that PV-UPQC mitigates the harmonics caused by nonlinear and maintains the THD of grid voltage, load voltage and grid current under limits of IEEE-519 standard. It can be seen that PV-UPQC is a good solution for modern distribution system by integrating

distributed generation with power quality improvement.

REFERENCES

[1] S.Devassy and B. Singh, "Modified p-q theory based control of solar PV integrated UPQC-S," in IEEE Industry Applications Society Annual Meeting, Oct 2016.

[2] Y. Yang, P. Enjeti, F. Blaabjerg, and H. Wang, "Wide-scale adoption of photovoltaic energy: Grid code modifications are explored in the distribution grid," *IEEE Ind. Appl. Mag.*, vol. 21, no. 5, pp. 21–31, Sept 2015.

[3] B. Singh, A. Chandra and K. A. Haddad, *Power Quality: Problems and Mitigation Techniques*. London: Wiley, 2015.

[4] M. Bollen and I. Guo, *Signal Processing of Power Quality Disturbances*. Hoboken: Johm Wiley, 2006.

[5] P. Jayaprakash, B. Singh, D. Kothari, A. Chandra, and K. Al-Haddad, "Control of reduced-rating dynamic voltage restorer with a battery energy storage system," *IEEE Trans. Ind. Appl.*, vol. 50, no. 2, pp. 1295–1303, March 2014.

[6] M. Badoni, A. Singh, and B. Singh, "Variable forgetting factor recursive least square control algorithm for DSTATCOM," *IEEE Trans. Power Del.*, vol. 30, no. 5, pp. 2353–2361, Oct 2015.

[7] A. Rauf and V. Khadkikar, "An enhanced voltage sag compensation scheme for dynamic voltage restorer," *IEEE Trans. Ind. Electron.*, vol. 62, no. 5, pp. 2683–2692, May 2015.

[8] V. Khadkikar, "Enhancing electric power quality using PV-UPQC: A comprehensive overview," *IEEE Trans. Power Electron.*, vol. 27, no. 5, pp. 2284–2297, May 2012.

[9] B. Han, B. Bae, H. Kim, and S. Baek, "Combined operation of unified power-quality conditioner with distributed generation," *IEEE Trans. Power Del.*, vol. 21, no. 1, pp. 330–338, Jan 2006.

[10] B. Singh, C. Jain, and S. Goel, "ILST control algorithm of single stage dual purpose grid connected solar pv system," *IEEE Trans. Power Electron.*, vol. 29, no. 10, pp. 5347–5357, Oct 2014.

[11] N. D. Tuyen and G. Fujita, "PV-active power filter combination supplies power to nonlinear load and compensates utility current," *IEEE Power and Energy Technology Systems Journal*, vol. 2, no. 1, pp. 32–42, March 2015.

[12] M. Davari, S. Ale-Emran, H. Yazdanpanahi, and G. Gharehpetian, "Modeling the combination of PV-UPQC and photovoltaic arrays with multi-input single-output dc-dc converter," in *IEEE/PES Power Systems Conference and Exposition, 2009. PSCE '09.*, March 2009, pp. 1–7.

[13] B. Subudhi and R. Pradhan, "A comparative study on maximum power point tracking techniques for photovoltaic power systems," *IEEE Transactions on Sustainable Energy*, vol. 4, no. 1, pp. 89–98, Jan 2013.

[14] L. Czarnecki, "Constraints of instantaneous reactive power p-q theory," *IET Power Electronics*, vol. 7, no. 9, pp. 2201–2208, September 2014.

[15] M. Kesler and E. Ozdemir, "Synchronous-reference-frame-based control method for PV-UPQC under unbalanced and distorted load conditions," *IEEE Trans. Ind. Electron.*, vol. 58, no. 9, pp. 3967–3975, Sept 2011.

[16] N. Tummuru, M. Mishra, and S. Srinivas, "Multifunctional VSC controlled microgrid using instantaneous symmetrical components theory," *IEEE Transactions on Sustainable Energy*, vol. 5, no. 1, pp. 313–322, Jan 2014.